

www.acsami.org Research Article

# Durable Liquid- and Solid-Repellent Elastomeric Coatings Infused with Partially Crosslinked Lubricants

Jing Wang, Bingyu Wu, Abhishek Dhyani, Taylor Repetto, Andrew J. Gayle, Tae H. Cho, Neil P. Dasgupta,\* and Anish Tuteja\*



Cite This: ACS Appl. Mater. Interfaces 2022, 14, 22466-22475



**ACCESS** I

Metrics & More



Article Recommendations



Supporting Information

coatings infused with partially crosslinked lubricants

<u>Lubricant</u> <u>Partially-Crosslinked</u>

Durable liquid-and-solid repellent elastomeric

Durable Anti-Fouling Coating

Solid Repellency

ABSTRACT: Surfaces that are resistant to both liquid fouling and solid fouling are critical for many industrial and biomedical applications. However, surfaces developed to address these challenges thus far have been generally susceptible to mechanical damage. Herein, we report the design and fabrication of robust solid- and liquid-repellent elastomeric coatings that incorporate partially crosslinked lubricating chains within a durable polymer matrix. In particular, we fabricated partially crosslinked omniphobic polyurethane (omni-PU) coatings that can repel a broad range of liquid and solid foulants. The fabricated coatings are an order of magnitude more resistant to cyclic abrasion than current state-of-the-art slippery surfaces. Further through the integration of classic wetting and tribology models, we introduce a new material design parameter  $(K_{AR})$  for abrasion-resistant polymeric coatings. This combination of mechanical durability and broad antifouling properties enables the implication of such coatings to a wide variety of industrial and medical settings, including biocompatible implants, underwater vehicles, and antifouling robotics.

KEYWORDS: wetting, omniphobicity, solid fouling, wear, mechanical properties, lubrication

## INTRODUCTION

Surfaces exposed to real-world conditions are often immersed in complex environments and are susceptible to fouling from both liquids and solids. Examples include biofouling in the maritime industry, 1-3 liquid condensation or frost formation on heat exchangers, 4-6 and bacterial infection on biomedical devices.<sup>7,8</sup> Surface fouling can seriously impact the performance of machines and human health. It is challenging to prevent these fouling processes because they may simultaneously involve multiple phases of foulants, which in turn can vary by orders of magnitude in terms of foulant modulus and fouling length-scales. 9,10

Over the past three decades, numerous liquid-repellent surfaces (e.g., superhydrophobic surfaces 11-13 and superoleophobic surfaces<sup>14–17</sup>) have been developed using micro/ nanoscale surface textures and low-surface-energy chemicals. These liquid-repellent surfaces can retain an air layer and form a liquid-solid-air composite interface, which can minimize the contact area between the liquid and solid phases. However, these surfaces cannot intrinsically repel solid foulants or multiphase foulant mixtures because the air layer that they rely on for liquid repellency can be displaced by a variety of solid foulants. 18-20 This removal of the air layer leads to a significant increase in the adhesion between the foulants and the surface as the underlying surface textures are filled. In addition, repellent surfaces based on the careful design of micro/nanostructures <sup>13,14</sup> can be easily damaged by mechanical abrasion or scratching.<sup>13</sup>

A few examples of surfaces that can repel a broad range of solid and liquid foulants have been developed recently.<sup>2</sup> These surfaces are designed to form a molecularly smooth surface using liquid lubricants or liquid-like polymer brushes, which can replace the solid-foulant interface with a liquidfoulant interface. However, these surfaces typically suffer from poor mechanical durability. 29,30 For example, slippery liquidinfused surfaces can be rendered dysfunctional by shear flow or mechanical abrasion.<sup>29,31</sup> The poor mechanical durability of such surfaces can be attributed to the loss of lubricant surface coverage during abrasion and the softness of the intermediate textured layer. These durability limitations prevent such surfaces from being widely implemented in industrial and biomedical settings.

Various approaches have been explored to enhance the mechanical durability of such slippery smooth surfaces, including regeneration of the lubricant or the underlying solid material texture, 32,33 use of composite materials, 13,34 or self-healing through thermal stimulation. 29,35 However, many of these methods have typically only resulted in moderate durability improvements, 29,32 while some studies have

Received: February 23, 2022 Accepted: April 26, 2022 Published: May 9, 2022





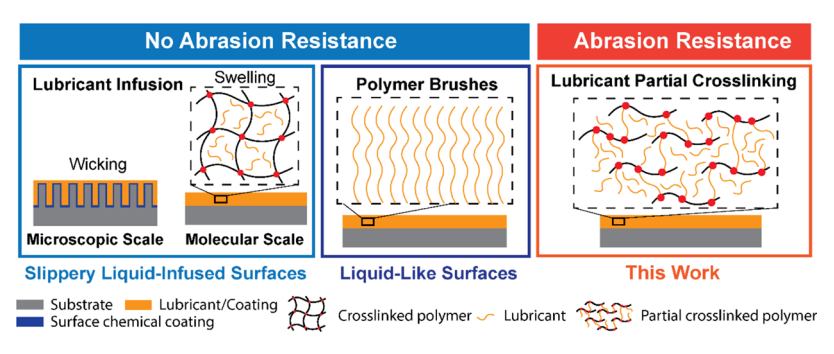


Figure 1. Schematic comparison of various surface coating strategies, including lubricant infusion, polymer brushes, and partial crosslinking of the lubricant within a polymer matrix.

demonstrated more improved abrasion resistance.<sup>34</sup> Thus, surfaces with improved abrasion resistance are needed to enable robust liquid and solid repellency in harsh working

Herein, we report the design and fabrication of mechanically durable elastomeric coatings that can repel a wide range of liquid and solid foulants. We also discuss a new design framework for developing such coatings by utilizing a modified classical tribology model, as well as the Hansen solubility parameters.<sup>36</sup> This design framework identifies the requirements for creating durable omniphobic coatings: a high coating hardness, complete lubrication, that is, lubrication that is retained even after mechanical abrasion, and a small Hansen solubility circle for the lubricant. Applying these design principles, we introduce a lubricant that is partially crosslinked within the polyurethane (PU) matrix to fabricate omniphobic polyurethane (omni-PU) elastomeric coatings that can withstand more than an order of magnitude increase in the number of harsh abrasion cycles, when compared to current state-ofthe-art omniphobic coatings. In addition to its favorable mechanical properties, omni-PU can repel liquids with a wide range of surface tensions from 12 to 72 mN/m. Furthermore, omni-PU is able to prevent solid fouling from different foulants with modulus spanning 7 orders of magnitude. Finally, because of the wide range of lubricant candidates that can be used to form omni-PU surfaces, the repellency and transparency of the coatings can be tailored for specific application requirements.

#### ■ RESULTS AND DISCUSSION

Design of Mechanically Durable Elastomeric Coatings. A classic wear model, known as the Ratner-Lancaster model,  $^{37,38}$  predicts that the wear rate  $(W_R)$  of a polymer, defined as the worn material volume per unit sliding distance, can be expressed as:

$$W_{\rm R} = C\mu/H\sigma\varepsilon \tag{1}$$

here C is a constant,  $\mu$  is the friction coefficient, H is the hardness of the polymer, and  $\sigma$  and  $\varepsilon$  are the stress and strain at tensile rupture. Based on this model, a polymeric coating with a low wear rate  $(W_R)$  should have a high yield strength and hardness, as well as a low friction coefficient with the abrader. The friction coefficient can be reduced by introducing lubrication, which can also enhance the yield strength of the interface.<sup>39</sup> For a lubricated surface, considering the deformation of the solid substrate during mechanical abrasion, the friction coefficient ( $\mu$ ) based on Hardy's friction model<sup>40</sup> can be expressed as:

$$\mu = (r \cdot s_1 + (1 - r) \cdot s_s)/H \tag{2}$$

where r is the ratio of lubricated area to total area,  $s_1$  and  $s_s$  are the shear strength of the lubricant film and the solid substrate respectively, and H is the hardness of the solid substrate. <sup>41,42</sup> In most cases,  $s_1$  is significantly lower in magnitude than  $s_s$ . For example, the shear strength of a lubricant film formed by polymer brushes is ~0.1 MPa, 43 which is at least 2 orders of magnitude smaller than the typical shear strength of ceramics and metals (10–1000 MPa). 44,45 Thus, the wear rate  $(W_R)$  can be expressed as:

$$W_{\rm R} = C[r \cdot s_1 + (1 - r) \cdot s_{\rm m}] / H^2 \sigma \varepsilon \tag{3}$$

Based on this modified relation for abrasive wear on polymeric coatings, a wear resistant coating can be achieved by: (1) maintaining a stable lubricant layer that remains on the surface both during and after abrasion (i.e., maintain  $r \sim 1$ ) and (2) utilizing a polymer matrix with high hardness (i.e., increase H).

Current state-of-the-art lubricated surfaces can be formed by two distinct methods: (1) infusing a lubricant into a porous matrix (Figure 1)<sup>2,21,22,25</sup> and (2) covalently attaching mobile polymer brushes (i.e., polymers above their glass transition temperature) onto smooth substrates (Figure 1). 23,24 Mechanical abrasion can easily result in removal of the lubricant layer and cause damage to liquid-infused slippery surfaces by exposing the unlubricated solid substrate (i.e., decreasing r). On the other hand, surfaces with mobile polymer brushes can be easily damaged by mechanical abrasion owing to the small thickness (~1 to 10 nm) and the softness of the polymer layer.46 Therefore, there is a need to develop coatings that are concurrently mechanically hard and maintain a stable lubrication layer.

Herein, we develop mechanically durable coatings where the lubricant is partially crosslinked within a hard elastomer as shown in Figure 1. This enables the coating to have a relatively high hardness and to maintain complete lubrication during and after abrasion, that is, retain  $r \sim 1$  and therefore a low  $W_R$ . In addition, this partial crosslinking of the lubricant within the elastomer matrix can also help reduce the loss of lubricant through shear flow, wear, and evaporation. 31,45

**Design of Durable PUs with**  $r \sim 1$ **.** Many PUs [including the PU elastomer used in this study, which is formed by aliphatic polyisocyanate (HDI trimer) crosslinking with hydroxyl-bearing polyester] exhibit high hardness (61 Shore A, Table S1) and wear-resistance.  $^{48-50}$  As a result, these PU materials are promising for use as a polymer matrix to form completely lubricated (i.e.,  $r \sim 1$  during and after abrasion) solid- and liquid-repellent coatings with enhanced mechanical durability. To achieve complete lubrication within the PU

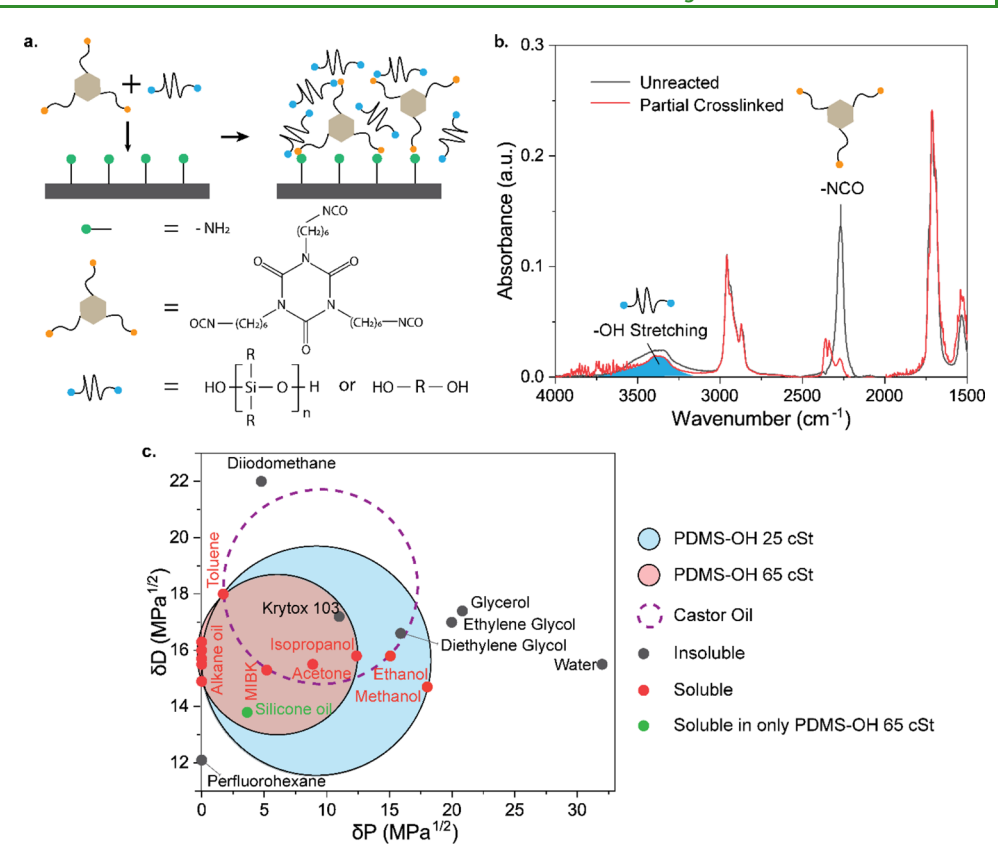


Figure 2. Design of omni-PU coatings. (a) Schematic illustrating the chemical reaction of the polyol and the HDI trimer to form omni-PU. The substrate was pretreated with amine-silane to enhance bonding with the omni-PU coating. (b) FTIR spectra of the unreacted omni-PU coating solution and partially crosslinked omni-PU. The polyol used here was hydroxyl polydimethylsiloxane (PDMS-OH). (c) Liquid repellency predictions using the Hansen solubility parameters. The circles are the Hansen solubility circles for the corresponding polyols.

elastomer, we reacted a number of different polyols (PDMS-OH with a viscosity of 25 cSt, PDMS-OH with a viscosity of 65 cSt, fluorinated PDMS diol (C7-F), and castor oil) with the HDI trimer (molecular structure shown in Figure 2a) to form a partially crosslinked polymer matrix, leaving the unreacted free polyol molecules as the lubricant both within and on top of the polymer (Figures 1 and 2a).

Here, we selected PDMS-OH with a viscosity of 25 cSt (PDMS-OH 25 cSt) as a model polyol to demonstrate the partial crosslinking of this modified PU. Before the isocyanate reaction, the Fourier-transform infrared spectroscopy (FTIR) spectrum of the coating solution (Figure 2b) exhibited a strong peak associated with the isocyanate group (-NCO group) from the HDI trimer. The spectrum also displayed hydroxyl (-OH group) stretching modes, which arise from the PDMS-OH 25 cSt. After the crosslinking reaction, the FTIR spectrum (Figure 2b) showed a significantly reduced isocyanate peak and a corresponding reduction in the peak associated with hydroxyl stretching, indicating the reaction between these two moieties as partial crosslinking occurs.

**Design of Omniphobicity.** The liquid repellency of mechanically durable PU coatings can be determined by considering the lubricant/polyol immiscibility with various contacting liquids. Therefore, we investigated the solubility of several polyols in a number of common polar and nonpolar liquids with surface tension spanning from 12 to 72 mN/m. Based on the solubility tests (see Table S3), Hansen solubility circles for the polyols were formed by plotting the dispersive  $(\delta D)$  and polar  $(\delta P)$  solubility parameters of the testing liquids, as shown in Figure 2c. The Hansen solubility circles

are defined as the minimal circular area that can encompass all of the liquids that are miscible with the corresponding polyols.<sup>36</sup> Therefore, they can serve as an effective predictor of the solubility and, thereby, the repellency of the omniphobic PU (omni-PU) coatings against specific contacting liquids as a function of the polyols used to form the lubricant. For example, PDMS-OH 25 cSt is represented by the light blue solubility circle in Figure 2c, which illustrates that it is miscible with different polar alcohols including ethanol and methanol. This predicts that the omni-PU with PDMS-OH 25 cSt cannot repel ethanol or methanol (Table S4). If these alcohols need to be repelled, then PDMS-OH with a higher molecular weight should be used as the partially crosslinked lubricant. An example of such a lubricant is PDMS-OH 65 cSt, whose solubility circle is also shown in Figure 2c.

This solubility design framework can aid in the selection of appropriate polyols to form omni-PU coatings that can repel a specific contacting liquid that may be present in a particular application. This adds a third design criterion for the fabrication of durable liquid and solid-repellent coatings: the partially crosslinked lubricants (polyols in this case) should have small solubility circles. For example, ethylene glycol has a solubility circle (Figure S1) that is much larger than the polyol circles in Figure 2c, and therefore, it is not useful to form omni-PU surfaces. Another example to highlight is castor oil, whose solubility circle is relatively small, but the resulting coatings are soft (hardness: 12 Shore A) and not mechanically durable. Thus, castor oil is not useful to form omni-PU surfaces because it does not satisfy the criteria for wear resistant coatings as discussed above.

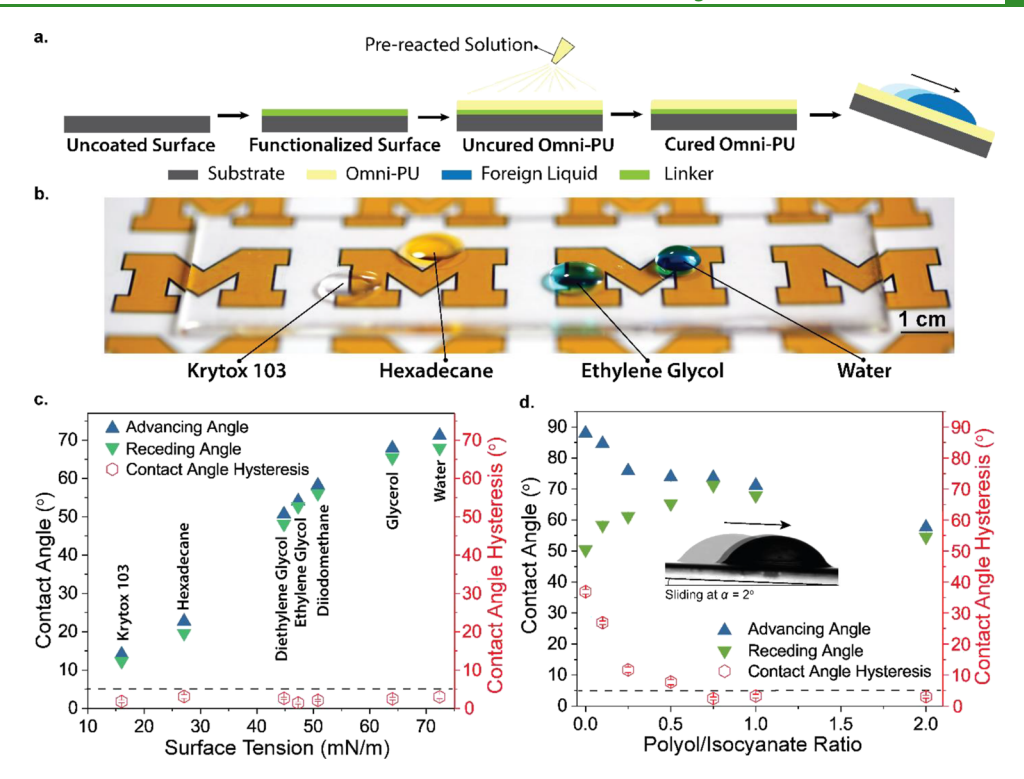


Figure 3. Fabrication of omni-PU coatings and their liquid repellency characterization. (a) Schematic illustration of the fabrication process for omni-PU. (b) Optical photograph showing omni-PU with PDMS-OH 25 cSt as the lubricant and its liquid repellency toward Krytox 103, hexadecane, ethylene glycol, and water. (c) Contact angle and contact angle hysteresis measurements on the omni-PU with different testing liquids, using a droplet volume of 5  $\mu$ L. (d) Contact angle and contact angle hysteresis measurements on omni-PU with varying the PDMS-OH 25 cSt to HDI trimer ratio. The testing liquid was 5  $\mu$ L of DI water. The error bars were obtained from at least five independent measurements.

For solid repellency, it has previously been shown that coatings with a stable lubrication layer are capable of repelling different solid foulants, including bacteria, <sup>51</sup> fecal waste, <sup>20</sup> marine foulant, <sup>2</sup> and ice. <sup>4</sup> Based on the stable lubrication layer formed on omni-PU, it is expected that omni-PU coatings would also have solid repellency in addition to liquid repellency, which is demonstrated in a later section.

Fabrication of Omni-PU Coatings. Based on the design criteria discussed above, we developed a facile, single-step spray-coating-based fabrication process for omni-PU coatings (Figure 3a). The polymeric coatings can be readily applied and cured on a variety of substrates, for example, glass as shown in Figure 3b. We selected PDMS-OH 25 cSt as a representative polyol to demonstrate the synthesis of omni-PU, because it has a relatively small solubility circle and can form hard omni-PU coatings (H = 42 Shore A). Because PDMS-OH 25 cSt is not directly miscible with the HDI trimer, we performed Hansen solubility analysis (Figure S2 and Supporting Information) and identified methyl isobutyl ketone (MIBK) as an appropriate solvent for both the crosslinkable lubricant (i.e., the polyol: PDMS-OH 25 cSt) and the HDI trimer. The optimal curing conditions for the PDMS-OH 25 cSt and HDI trimer were determined by varying the amount of catalyst present and the reaction temperature (20–100 °C) (Figure S3).

Liquid Repellency of Omni-PU. Omni-PU coatings were fabricated with various lubricants (PDMS-OH 25 cSt, PDMS-OH 65 cSt, and C7-F), and their advancing and receding contact angles were measured against a variety of contacting liquids. The samples were shown to successfully repel liquids with a wide range of surface tensions from 12 to 72 mN/m (Figure 3b,c, and Table S4).

The premixed polyol percentage in the coating solution was also systematically varied. The results demonstrated that the weight ratio between the polyol and the isocyanate must be  $\geq 0.75$  to achieve strong liquid repellency, that is, an ultralow contact angle hysteresis (<5°), toward different contacting liquids (Figure 3d). The free polyol molecule percentage in omni-PU can be varied by tuning the premixed ratio of the polyol and the HDI trimer (Table S5). For example, a 2:1 weight ratio of the polyol and the HDI trimer resulted in  $\sim 20$  wt % of free oils throughout the volume and top surface of the resulting omni-PU film (further details in the Supporting Information).

Furthermore, our experiments show that the Hansen solubility design framework is >80% accurate (i.e., three exceptions in 17 different tested solvents) when predicting the liquid repellency for omni-PU with PDMS-OH 25 cSt. As an example of one of these exceptions, the Hansen solubility parameters of Krytox oil and hexadecane are within the solubility circle of the PDMS-OH 25 cSt, but they can still be repelled by omni-PU. The mechanisms of the repellency toward these two liquids are different. Krytox oil is not soluble with PDMS-OH 25 cSt (Table S3), although its Hansen solubility parameters fall within the solubility circle. For hexadecane, it is soluble with PDMS-OH 25 cSt, but only after sonication (Table S3). Contact angle measurements only require a short contact time (a few minutes). It is likely that the two liquids remained immiscible over these short time scales (Figure S4). Note that the Hansen solubility circle/ sphere methodology does not account for partial miscibility between solvents, and this limitation contributes at least partially to the exceptions described here.

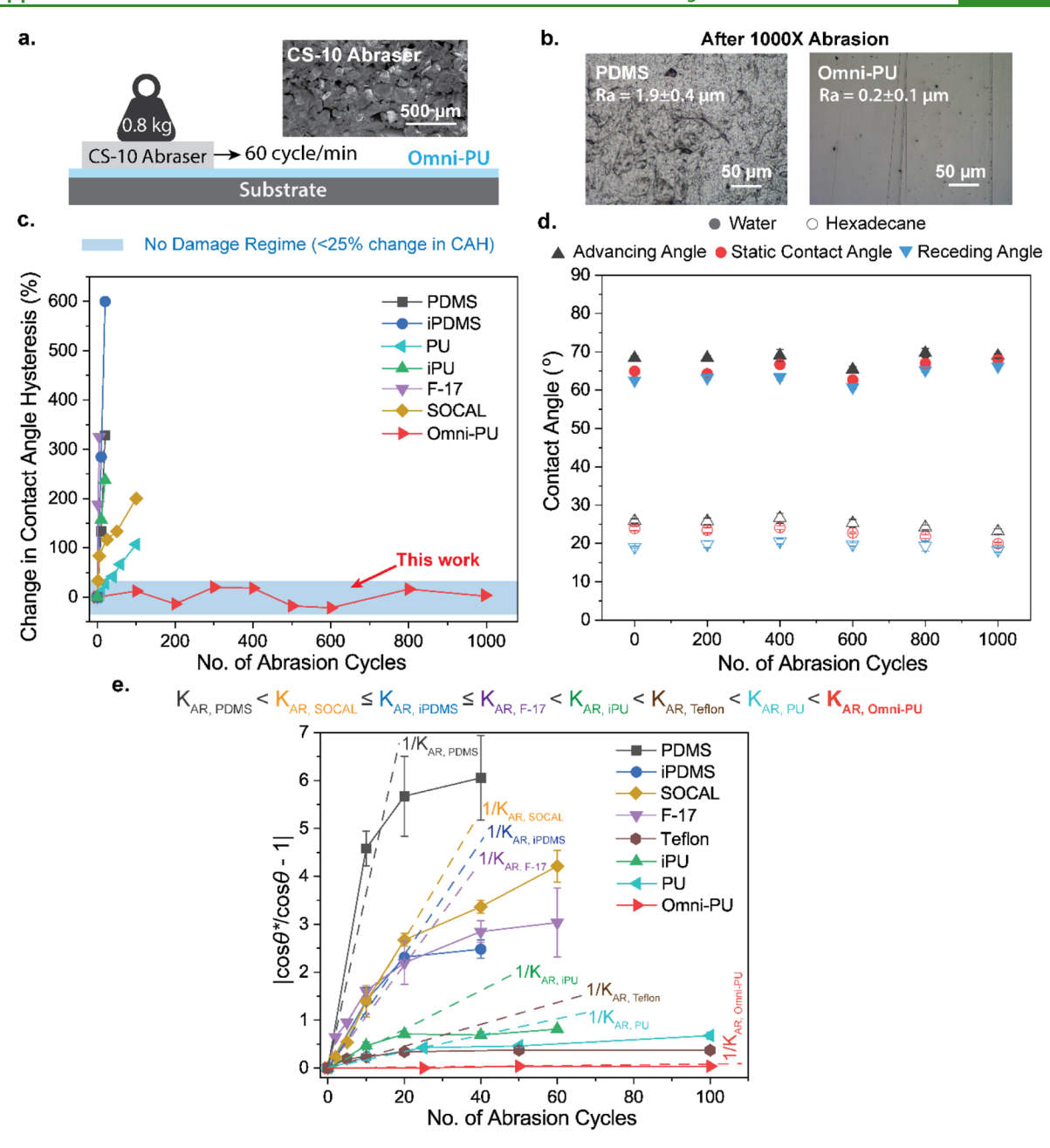


Figure 4. Abrasion resistance of omni-PU and state-of-the-art controls. (a) Schematic of the Taber abrasion test, including a scanning electron microscopy (SEM) image showing the topography of the CS-10 abrader. (b) Surface roughness measurements of omni-PU and PDMS films after 1000 cycles of mechanical abrasion. The error bars were obtained from at least three independent measurements. (c) Change in contact angle hysteresis for water droplets (5  $\mu$ L) on omni-PU with a polyol-to-HDI-trimer ratio of 1:1 and the control surfaces throughout the Taber abrasion tests. (d) Advancing contact angle, static contact angle, and receding contact angle measurements with water and hexadecane (5  $\mu$ L) on omni-PU throughout the Taber abrasion tests. (e) Value of loos  $\theta$ \*/cos  $\theta$  – 1| vs number of abrasion cycles for omni-PU and various control surfaces. The error bars were obtained from at least five independent measurements.

In addition to their liquid repellency, the omni-PU coatings with PDMS-OH 25 cSt are highly transparent, with an optical transmittance of >90% across the visible spectrum (Figure S5). This makes them attractive coatings for windows or other optical surfaces. For applications that do not require optical transparency, the HDI trimer can be reacted with multiple immiscible polyols (e.g., PDMS-OH and hydroxyl-bearing polyester) to form omni-PU. These systems are opaque but can still maintain a stable lubrication layer and demonstrate the same liquid repellency performance as the transparent omni-PU systems (Figure S6).

**Mechanical Durability of Omni-PU.** To test the mechanical durability of the omni-PU, Taber abrasion testing was performed, which is similar to the ASTM F3300–18 standard for measuring durability (details in the Experimental Section). The test utilizes a harsh abrasive surface (in this case we used the CS-10 abrader, which is composed of  $Al_2O_3$  particles embedded in rubber), which contacts the coating using a linear cyclic motion under a high applied load (~8.3 N), as shown in Figures 4a and S7. A durable and commercially available PU (HDI trimer crosslinking with hydroxyl-bearing polyester, H = 61 Shore A) without any partially crosslinked lubricant can withstand >1000 cycles of

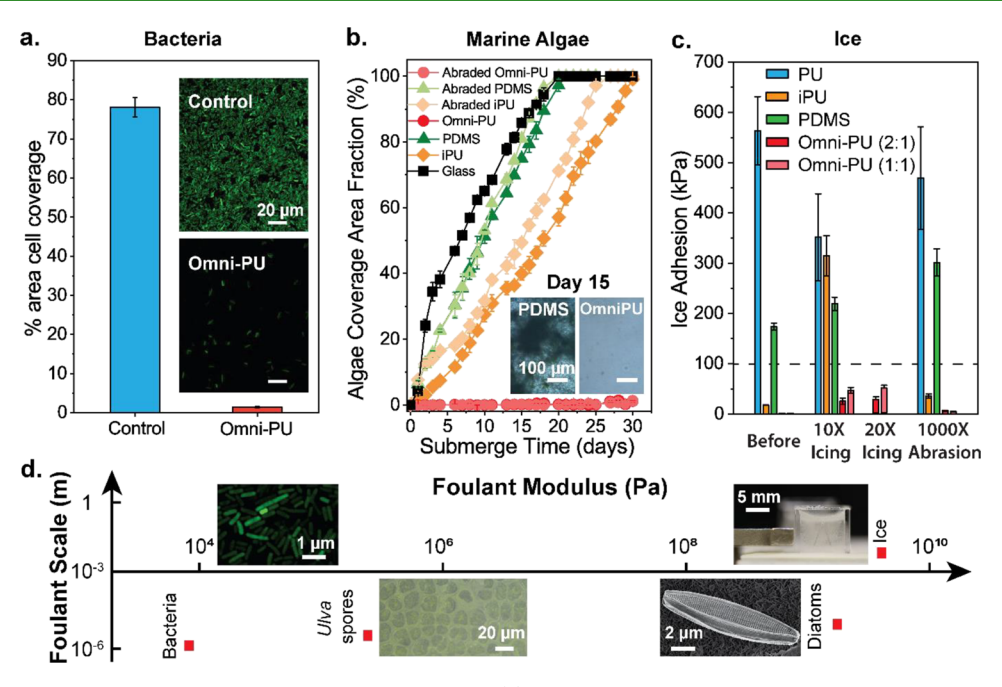


Figure 5. Solid fouling tests on omni-PU and various control surfaces. (a) *E. coli* adhesion on omni-PU and PU surfaces. The inset fluorescent images compare the attached bacterial coverage of the surfaces. (b) Algae coverage area fraction on the omni-PU and control surfaces with and without abrasion (PU, iPU, PDMS, and glass) over a period of 30 days. Optical microscopy images comparing the omni-PU and control surfaces after 15 days of algal fouling. (c) Ice adhesion strength on various surfaces before and after durability testing (cyclic icing/deicing and mechanical abrasion). (d) Summary chart illustrating the repellency of omni-PU to solid foulants with a wide range of elastic moduli. The inset images from left to right are a microscopic fluorescent image of *E. coli*, a microscopic image of *Ulva fasciata* cells containing spores, a SEM image of a diatom, and an optical image of an ice block being pushed by a force gauge probe. The error bar was obtained from at least three independent measurements.

mechanical abrasion with minimal weight loss (<0.2 wt %). In contrast, a softer polymer such as PDMS (Sylgard 184 10:1, H = 42 Shore A) decreases by  $\sim5\%$  in weight after the same abrasion process.

Owing to the ability of omni-PU to maintain complete lubrication  $(r \sim 1)$ , the abrasion resistance of the material is further enhanced when compared to the nonlubricated PU surface. Optical microscopy analysis of the omni-PU and a variety of control surfaces [i.e., PDMS, PDMS swelled with silicone oil (iPDMS),<sup>2</sup> PU, and PU swelled with PDMS-OH (iPU); additional details in the Supporting Information are shown in Figure S8, which illustrates the differences in surface morphology before and after abrasion. iPDMS and iPU surfaces were chosen as representative liquid-infused, liquid and solid repellent polymeric coatings developed in the recent literature. 2,53,54 Obvious scratches and surface roughening were observed after mechanical abrasion on all of the control surfaces. In contrast, the omni-PU surface showed only few minor scratches. Based on roughness measurements that were captured using optical profilometry before and after abrasion (Figure 4b and Table S6), the omni-PU surfaces exhibited a mild change in surface roughness (from 29 to 195 nm), while the roughness on the control surfaces experienced a significantly greater increase. For example, the surface roughness of the PDMS surface increased from 43 to 1914 nm after abrasion.

To quantify the influence of surface abrasion on the liquid repellency of the various coatings, we performed contact angle and contact angle hysteresis measurements as a function of abrasion cycles. The contact angle hysteresis for all of the control coatings, including PU, PDMS, perfluorinated silanized silicon (F-17), PDMS brushes (SOCAL),<sup>24</sup> iPDMS, and iPU, increased significantly after abrasion (between 100 and 600%

after 100 cycles of Taber abrasion; see Figures 4c and S9). In contrast, the omni-PU maintained its low contact angle hysteresis with minimal changes in hysteresis even after 1000 cycles of mechanical abrasion (Figure 4c,d). Overall, the omni-PU outperforms all state-of-the-art liquid-repellent surfaces in the mechanical abrasion tests, retaining its liquid repellency after more than an order of magnitude increase in the number of abrasion cycles.

Abrasion Resistance Parameter for Polymeric Coatings. The Wenzel relation can be utilized to characterize how mechanical abrasion impacts the surface wetting properties. In particular, the newly generated surface area  $(\Delta A)$  from abrasive wear can be quantified using the Wenzel relation as:

$$\Delta A = RL_0 \cdot (\cos \theta^* / \cos \theta - 1) \tag{4}$$

where  $\theta^*$  is the contact angle after abrasion,  $\theta$  is the Young's contact angle, 2R is the width of the abrader, and  $L_0$  is the sliding distance of the abrader for each cycle (see details in the Supporting Information). In Taber abrasion, particularly when using ceramic particles embedded in rubber as the abrader (e.g., a CS-10 abrader), the newly generated surface area ( $\Delta A$ ) can be expressed as:  $\Delta A \propto L_0 \cdot N \cdot W_R$  (see details in the Supporting Information).

By combining the Wenzel relation and the modified Ratner–Lancaster correlation (i.e., eq 3), we can describe the correlation between the number of abrasion cycles (N) and the measured contact angles as (see the Supporting Information):

$$(\cos \theta^*/\cos \theta - 1) \propto N/K_{AR} \tag{5}$$

where we define  $K_{AR}$  to be the abrasion resistance parameter of the material, given as:

$$K_{AR} = \frac{H^2 \varepsilon \sigma}{r \cdot s_1 + (1 - r) \cdot s_m} \tag{6}$$

The higher the value of  $K_{AR}$ , the more durable the coating.

Based on eq 5, we estimated the  $K_{\rm AR}$  values for the different coatings in this work by performing contact angle measurements after various numbers of abrasion cycles. In particular, the water receding contact angle was measured for both the nonabraded and abraded coatings. The correlation between l  $\cos\theta^*/\cos\theta-1$  and the number of abrasion cycles (N) can be plotted as shown in Figure 4e. The initial slope of this plot varies approximately linearly with  $1/K_{\rm AR}$ . Accordingly, as the slope decreases, the abrasion resistance of the surface increases.

From this plot, it is clear that omni-PU ( $K_{AR} = 9070$ ) has the lowest slope and is therefore the most abrasion-resistant material tested. By analyzing the data in Figure 4e, we observe that iPDMS ( $K_{AR} = 12$ ) is more durable than PDMS ( $K_{AR} = 6$ ), which is due to the decrease of the friction coefficient ( $\mu$ ). Interestingly, the iPDMS and SOCAL (PDMS brushed:  $K_{AR} \sim 10$ ; see Table S7) surfaces have similar  $K_{AR}$  values, which is likely due to the presence of mobile chains on both surfaces. Based on eq 6, we could further compare the abrasion resistance of different coatings, when all relevant physical properties [e.g., hardness H, and the stress, strain at tensile rupture ( $\sigma$  and  $\varepsilon$ ), and the shear strength of the lubricant film and the solid substrate ( $s_1$  and  $s_s$ )] are known or measured.

**Solid Repellency of Omni-PU.** In addition to liquid repellency, we also tested the solid repellency of omni-PU against infectious bacteria (*Escherichia coli.*), soft marine foulants (cyanobacteria and diatom), and ice (Figure 5). To test bacterial adhesion, omni-PU surfaces and unmodified PU surfaces were exposed to a liquid culture of genetically modified *E. coli* with green fluorescent protein. After fouling, less than 3% of the area on the omni-PU samples was covered with *E. coli*, while ~80% of the area on the control surfaces was covered with biofilms (Figure 5a). These differences are attributed to the presence of a robust lubrication layer that remains adhered to the surface, <sup>51</sup> demonstrating that the omni-PU surfaces are highly efficient in preventing fouling from *E. coli*.

To evaluate fouling in a simulated marine algae environment, omni-PU was compared to a range of control surfaces (PDMS, iPU, and glass), both before and after 1000 cycles of Taber mechanical abrasion. Following our previously reported procedure,<sup>55</sup> the samples were submerged into the algae culture media, and the area covered by algae foulants (the algae coverage area fraction shown in Figure 5b) was quantified using optical microscopy every day for 30 days. The marine algae culture contained both soft (e.g., cyanobacteria) and hard (e.g., diatoms) solid foulants, with a range in elastic modulus from 10 to 106 kPa. 9,55 Both the abraded and the nonabraded omni-PU surfaces exhibited strong antifouling performance throughout the duration of the tests, outperforming the control surfaces, which were all fouled significantly within 20 days (100% coverage for PDMS and glass, and ~60% coverage for iPU) (Figure 5b). This antifouling performance is superior to previous reports using nanostructured superhydrophobic surfaces under the same algal fouling conditions (23 days of antifouling)<sup>55</sup> as well as slippery liquid-infused porous surfaces under similar marine fouling conditions (Ulva linza spores, 8 days of antifouling). 56 The excellent antifouling performance of omni-PU is attributed to the low adhesion between algae<sup>56</sup> and the PDMS-OH lubrication layer. The abraded PDMS and iPU

coatings experienced more fouling than the corresponding nonabraded surfaces. This is because abrasion results in a larger contact area (Table S6) for algae to settle and grow. In contrast, mechanical abrasion had a limited impact on the algal fouling on the omni-PU surfaces, because the surface roughness only increased slightly after abrasion (from 29 to 195 nm) and the coating remained completely lubricated (Figure 5b).

In addition, we tested marine fouling using a single-species solution containing *Ulva* spores (modulus: ~0.1 MPa) on both omni-PU and control surfaces (see in the Supporting Information). The *Ulva* spores preferentially accumulated on the control surface instead of the omni-PU surface (Figure S10). In addition to the low adhesion, the PDMS-OH layer on omni-PU can also influence the mechanosensing ability of the *Ulva* spores, <sup>57</sup> and is a likely contributor to the antifouling properties of the omni-PU surfaces.

In addition to biofouling, we also studied the adhesion behavior of ice, which is of significant importance in applications ranging from wind turbines to airplane wings. In these tests, omni-PU surfaces with varying polyol-to-HDI-trimer ratios (1:1 and 2:1) were compared with a range of control surfaces (PU, iPU, and PDMS) using a previously published ice cube adhesion test procedure (see Figure S11 and Supporting Information). S5,49,58 Icephobic surfaces generally are defined as having an ice adhesion strength below 100 kPa (the dashed line in Figure 5c). Prom Figures 5c and S11, before any cyclic abrasion, the lubricated surfaces were icephobic with an ice adhesion strength <30 kPa, while the other nonlubricated polymer coatings were not icephobic and had significantly higher ice adhesion strengths (up to 560 kPa).

To quantify the durability of omni-PU surfaces toward ice adhesion, we performed two tests: (1) multiple icing and deicing cycles and (2) ice adhesion after Taber mechanical abrasion. In particular, we performed 10 icing and deicing cycles on the omni-PU and control surfaces and measured their ice adhesion strengths after each cycle (Figures 5c and S12). The nonlubricated polymer surfaces (i.e., PDMS and PU) retained a high adhesion strength to ice throughout our testing. The lubricant layer on the iPU surfaces was almost completely removed after 10 icing cycles, resulting in a significant increase in ice adhesion strength from <30 to >300 kPa with multiple icing—deicing cycles. In comparison, the omni-PU surfaces remained icephobic with an ice adhesion strength below 50 kPa after 10 icing—deicing cycles.

Furthermore, we performed another 10 icing and deicing cycles on omni-PU surfaces with two different polyol-to-HDI-trimer ratios (1:1 and 2:1). The ice adhesion strength on these surfaces gradually increased to a plateau value of 33 and 51 kPa on omni-PU with polyol-to--HDI-trimer ratios of 2:1 and 1:1, respectively. This trend suggests that the omni-PU transitioned from displaying hydrodynamic lubrication to interfacial slippage <sup>49,59</sup> with ice during the first 20 cycles of icing-deicing (Figure S10).

We also measured the ice adhesion strength on these surfaces after 1000 cycles of Taber mechanical abrasion. As shown in Figure 5c, the ice adhesion strength remained relatively high ( $\sim$ 500 kPa) and unchanged on the durable PU surface. The ice adhesion strength on the abraded PDMS increased from  $\sim$ 170 to  $\sim$ 300 kPa, as the roughness of PDMS increased significantly after abrasion (Table S6). In contrast, mechanical abrasion had a more limited impact on the lubricated surfaces, including the partially lubricated iPU. The

ice adhesion strength only increased slightly on these surfaces, from 20 to 45 kPa on the iPU surface and from <1 to 10 kPa on the omni-PU surface, as shown in Figure 5c.

#### CONCLUSIONS

In summary, this study introduced three design principles for the fabrication of durable solid- and liquid-repellent surfaces: (1) Maintaining a stable lubricant layer before and after abrasion; (2) Utilizing an elastomer with a high hardness; and (3) Selecting a crosslinkable lubricant with a small Hansen solubility circle. We also integrated classic tribology and wetting models to introduce an abrasion resistance parameter  $(K_{AR})$ . Based on this understanding, we fabricated multiple mechanically durable omni-PU coatings, using a novel polyol reactive infusion method. These fabricated coatings could repel virtually all high and low surface tension liquids. Additionally, the coatings demonstrated a robust antifouling response toward various solid foulants, spanning a broad range of elastic moduli (1 kPa to 1 GPa) and geometric dimensions (micrometers to centimeters) (Figure 5d). As a result of these combined properties of abrasion resistance, liquid and solid repellency, and optical transparency, the omni-PU coatings can enable new applications in a variety of industrial and medical settings that may not be possible using current state-of-the-art materials.

#### EXPERIMENTAL SECTION

**Materials and Fabrication of Omni-PU.** Omni-PU with reactive oil infusion (hydroxy-terminated PDMS) was manufactured using multiple steps: 1. Vortex mixing of hydroxy-terminated polydimethylsiloxane (PDMS-OH) (Sigma-Aldrich) and HDI trimer (Covestro, Desmodur N3800) in a MIBK (Fisher Scientific) solvent for 15 min until the mixture has no bubbles and is optically clear. 2. Addition of a catalyst (dibutyltin dilaurate (Fisher Scientific) 0.1 wt % in MIBK) to the solution with a weight percentage of 2.67% followed by 5 min of vortex mixing and 10 min of sonication to remove bubbles. 3. Heating of the solution to 90 °C in the oven for 90 min. 4. Drop casting or spray coating the solution onto surfaces that were functionalized with -NH<sub>2</sub> groups before the coating process. Surface hydroxylation was performed using oxygen plasma exposure for 15 min with a power of 40 W.

Amine surface functionalization on glass was performed through the following process: the glass surface was exposed to an oxygen plasma for 15 min with a power of 40 W. Then the glass was placed into a solution of 2 wt % bis(3-trimethoxysilylpropyl) amine (Gelest Inc.) in ethanol (12.5 mL ethanol, 195  $\mu$ L silane, 0.63 mL of pH = 2 acetic acid solution; stirred for 2 h before use) for 20 min. 5. The coating was cured in a vacuum oven at 40–60 °C for a maximum of 2 days. 6. Postannealing of the coating was performed on a hot plate at a temperature of 60–75 °C for a maximum of 1 day. Note: The HDI trimer (Figure 2a) used here is highly sensitive to moisture.  $^{60}$ 

Materials and Fabrication of Control Surfaces. The control surfaces included glass, PDMS, PU, iPDMS, iPU, SOCAL, and F-17. A microscope glass slide was used from Fisher Scientific. Sylgard 184 (10:1) PDMS (Dow Inc) was cured in an oven at 80 °C for 24 h. To fabricate PU, HDI trimer (N3800 from Covestro) and hydroxylbearing polyester (670BA from Covestro) were cured in ambient air. iPDMS was fabricated by swelling PDMS (Sylgard 10:1) in silicone oil (20 cSt, Sigma-Aldrich) at 60 °C for 24 h. iPU was fabricated by submerging PU in PDMS-OH 25 cSt at 60 °C for 24 h.

**Taber Abrasion Test.** The Taber abrasion test was performed using a 5750 linear abrader from Taber Industries. We used the maximum abrasion speed 60 cycles/min with 100 mm travel distance per cycle, a harsh abrader (CS-10), and high loading weight (850 grams). The abrader was roughened following the instructions from

Taber Industries before all abrasion tests. Each Taber abrasion test used a newly prepared abrader.

## ASSOCIATED CONTENT

## **Solution** Supporting Information

The Supporting Information is available free of charge at https://pubs.acs.org/doi/10.1021/acsami.2c03408.

Experimental details for mechanical, chemical, and wetting characterization of omni-PU coatings and solid fouling tests on different coatings and derivation of abrasion resistance parameters (PDF)

#### AUTHOR INFORMATION

## **Corresponding Authors**

Neil P. Dasgupta — Department of Mechanical Engineering and Department of Materials Science and Engineering, University of Michigan, Ann Arbor, Michigan 48109, United States; orcid.org/0000-0002-5180-4063;

Email: ndasgupt@umich.edu

Anish Tuteja — Department of Materials Science and Engineering, Macromolecular Science and Engineering, Department of Chemical Engineering, and BioInterface Institute, University of Michigan, Ann Arbor, Michigan 48109, United States; orcid.org/0000-0002-2383-4572; Email: atuteja@umich.edu

#### **Authors**

Jing Wang — Department of Mechanical Engineering, University of Michigan, Ann Arbor, Michigan 48109, United States; Occid.org/0000-0002-7757-1261

Bingyu Wu – Department of Materials Science and Engineering and BioInterface Institute, University of Michigan, Ann Arbor, Michigan 48109, United States

Abhishek Dhyani – Macromolecular Science and Engineering and BioInterface Institute, University of Michigan, Ann Arbor, Michigan 48109, United States

Taylor Repetto – Department of Materials Science and Engineering and BioInterface Institute, University of Michigan, Ann Arbor, Michigan 48109, United States

Andrew J. Gayle – Department of Mechanical Engineering, University of Michigan, Ann Arbor, Michigan 48109, United States

Tae H. Cho – Department of Mechanical Engineering, University of Michigan, Ann Arbor, Michigan 48109, United States

Complete contact information is available at: https://pubs.acs.org/10.1021/acsami.2c03408

#### **Author Contributions**

J.W., N.P.D., and A.T. conceived the idea and designed the study. J.W. and B.W. prepared the sample. J.W., N.P.D., and A.T. conducted the materials design. J.W. conducted wetting design and characterization. J.W. and A.D. conducted the abrasion tests. J.W. and A.D. conducted the ice adhesion tests. T.R. performed the bacteria fouling tests. J.W. conducted the marine fouling tests. T.H.C. and A.J.G. conducted the surface roughness measurements. J.W. and A.J.G. conducted mechanical property tests. J.W., B.W., A.D., T.R., N.P.D., and A.T. analyzed and interpreted the result. J.W., N.P.D., and A.T. wrote the manuscript with the inputs from all authors.

#### Notes

The authors declare no competing financial interest.

#### ACKNOWLEDGMENTS

This work was supported by DARPA Young Faculty Award D18AP00066. Any opinions, findings, conclusions, or recommendations expressed in this publication are those of the authors and do not necessarily reflect the views of DARPA. This material is based upon work supported by the National Science Foundation under grant no. 1751590. We also thank Dr. Paul Armistead, Dr. Kathy Wahl, and the Office of Naval Research (ONR) for financial support under grant N00014-20-1-2817. The authors thank Prof. M. D. Thouless from the University of Michigan for valuable discussions.

#### REFERENCES

- (1) Callow, J. A.; Callow, M. E. Trends in the development of environmentally friendly fouling-resistant marine coatings. *Nat. Commun.* **2011**, *2*, 244.
- (2) Amini, S.; Kolle, S.; Petrone, L.; Ahanotu, O.; Sunny, S.; Sutanto, C. N.; Hoon, S.; Cohen, L.; Weaver, J. C.; Aizenberg, J.; Vogel, N.; Miserez, A. Preventing mussel adhesion using lubricant-infused materials. *Science* **2017**, *357*, *668*–*673*.
- (3) Sommer, S.; Ekin, A.; Webster, D. C.; Stafslien, S. J.; Daniels, J.; VanderWal, L. J.; Thompson, S. E. M.; Callow, M. E.; Callow, J. A. A preliminary study on the properties and fouling-release performance of siloxane—polyurethane coatings prepared from poly-(dimethylsiloxane) (PDMS) macromers. *Biofouling* **2010**, *26*, 961—972.
- (4) Kreder, M. J.; Alvarenga, J.; Kim, P.; Aizenberg, J. Design of anticing surfaces: smooth, textured or slippery? *Nat. Rev. Mater.* **2016**, *1*, 15003.
- (5) Cho, H. J.; Preston, D. J.; Zhu, Y.; Wang, E. N. Nanoengineered materials for liquid-vapour phase-change heat transfer. *Nat. Rev. Mater.* **2016**, *2*, 16092.
- (6) Dai, X.; Sun, N.; Nielsen, S. O.; Stogin, B. B.; Wang, J.; Yang, S.; Wong, T.-S. Hydrophilic directional slippery rough surfaces for water harvesting. *Sci. Adv.* **2018**, *4*, No. eaaq0919.
- (7) Banerjee, I.; Pangule, R. C.; Kane, R. S. Antifouling Coatings: Recent Developments in the Design of Surfaces That Prevent Fouling by Proteins, Bacteria, and Marine Organisms. *Adv. Mater.* **2011**, 23, 690–718.
- (8) Arciola, C. R.; Campoccia, D.; Montanaro, L. Implant infections: adhesion, biofilm formation and immune evasion. *Nat. Rev. Microbiol.* **2018**. *16*. 397–409.
- (9) Halvey, A. K.; Macdonald, B.; Dhyani, A.; Tuteja, A. Design of surfaces for controlling hard and soft fouling. *Philos. Trans. R. Soc. A* **2019**, 377, No. 20180266.
- (10) Dhyani, A.; Wang, J.; Halvey, A. K.; Macdonald, B.; Mehta, G.; Tuteja, A. Design and applications of surfaces that control the accretion of matter. *Science* **2021**, *373*, No. eaba5010.
- (11) Lafuma, A.; Quéré, D. Superhydrophobic states. *Nat. Mater.* 2003, 2, 457–460.
- (12) Wang, S. T.; Liu, K. S.; Yao, X.; Jiang, L. Bioinspired Surfaces with Superwettability: New Insight on Theory, Design, and Applications. *Chem. Rev.* **2015**, *115*, 8230–8293.
- (13) Wang, D.; Sun, Q.; Hokkanen, M. J.; Zhang, C.; Lin, F.-Y.; Liu, Q.; Zhu, S.-P.; Zhou, T.; Chang, Q.; He, B.; Zhou, Q.; Chen, L.; Wang, Z.; Ras, R. H. A.; Deng, X. Design of robust superhydrophobic surfaces. *Nature* **2020**, *582*, 55–59.
- (14) Tuteja, A.; Choi, W.; Ma, M.; Mabry, J. M.; Mazzella, S. A.; Rutledge, G. C.; McKinley, G. H.; Cohen, R. E. Designing Superoleophobic Surfaces. *Science* **2007**, *318*, 1618–1622.
- (15) Deng, X.; Mammen, L.; Butt, H. J.; Vollmer, D. Candle Soot as a Template for a Transparent Robust Superamphiphobic Coating. *Science* **2012**, 335, 67–70.
- (16) Liu, T.; Kim, C.-J. Turning a surface superrepellent even to completely wetting liquids. *Science* **2014**, *346*, 1096–1100.

- (17) Tuteja, A.; Choi, W.; Mabry, J. M.; McKinley, G. H.; Cohen, R. E. Robust omniphobic surfaces. *Proc. Natl. Acad. Sci. U. S. A.* **2008**, 105, 18200–18205.
- (18) Kulinich, S. A.; Farhadi, S.; Nose, K.; Du, X. W. Superhydrophobic Surfaces: Are They Really Ice-Repellent? *Langmuir* **2011**, 27, 25–29.
- (19) Hwang, G. B.; Page, K.; Patir, A.; Nair, S. P.; Allan, E.; Parkin, I. P. The Anti-Biofouling Properties of Superhydrophobic Surfaces are Short-Lived. *ACS Nano* **2018**, *12*, 6050–6058.
- (20) Wang, J.; Wang, L.; Sun, N.; Tierney, R.; Li, H.; Corsetti, M.; Williams, L.; Wong, P. K.; Wong, T.-S. Viscoelastic solid-repellent coatings for extreme water saving and global sanitation. *Nat. Sustain.* **2019**, *2*, 1097–1105.
- (21) Wong, T.-S.; Kang, S. H.; Tang, S. K. Y.; Smythe, E. J.; Hatton, B. D.; Grinthal, A.; Aizenberg, J. Bioinspired self-repairing slippery surfaces with pressure-stable omniphobicity. *Nature* **2011**, *477*, 443–447
- (22) Lafuma, A.; Quéré, D. Slippery pre-suffused surfaces. EPL 2011, 96, 56001.
- (23) Cheng, D. F.; Urata, C.; Yagihashi, M.; Hozumi, A. A Statically Oleophilic but Dynamically Oleophobic Smooth Nonperfluorinated Surface. *Angew. Chem. Int. Ed.* **2012**, *51*, 2956–2959.
- (24) Wang, L.; McCarthy, T. J. Covalently Attached Liquids: Instant Omniphobic Surfaces with Unprecedented Repellency. *Angew. Chem. Int. Ed.* **2016**, *55*, 244–248.
- (25) Lv, J.; Yao, X.; Zheng, Y.; Wang, J.; Jiang, L. Antiadhesion organogel materials: from liquid to solid. *Adv. Mater.* **2017**, *29*, No. 1703032.
- (26) Rabnawaz, M.; Liu, G.; Hu, H. Fluorine-Free Anti-Smudge Polyurethane Coatings. *Angew. Chem. Int. Ed.* **2015**, *54*, 12722–12727.
- (27) Monga, D.; Guo, Z.; Shan, L.; Taba, S. A.; Sarma, J.; Dai, X. Quasi-Liquid Surfaces for Sustainable High-Performance Steam Condensation. *ACS Appl. Mater. Interfaces* **2022**, *14*, 13932–13941.
- (28) Chen, Y.; Yu, X.; Chen, L.; Liu, S.; Xu, X.; Zhao, S.; Huang, S.; Tian, X. Dynamic Poly(dimethylsiloxane) Brush Coating Shows Even Better Antiscaling Capability than the Low-Surface-Energy Fluorocarbon Counterpart. *Environ. Sci. Technol.* **2021**, *55*, 8839–8847.
- (29) Wang, J.; Kato, K.; Blois, A. P.; Wong, T.-S. Bioinspired omniphobic coatings with a thermal self-repair function on industrial materials. *ACS Appl. Mater. Interfaces* **2016**, *8*, 8265–8271.
- (30) Tian, X.; Verho, T.; Ras, R. H. Moving superhydrophobic surfaces toward real-world applications. *Science* **2016**, *352*, 142–143.
- (31) Wexler, J. S.; Jacobi, I.; Stone, H. A. Shear-driven failure of liquid-infused surfaces. *Phys. Rev. Lett.* **2015**, *114*, No. 168301.
- (32) Manna, U.; Lynn, D. M. Restoration of Superhydrophobicity in Crushed Polymer Films by Treatment with Water: Self-Healing and Recovery of Damaged Topographic Features Aided by an Unlikely Source. *Adv. Mater.* **2013**, *25*, 5104–5108.
- (33) Cui, J.; Daniel, D.; Grinthal, A.; Lin, K.; Aizenberg, J. Dynamic polymer systems with self-regulated secretion for the control of surface properties and material healing. *Nat. Mater.* **2015**, *14*, 790–795.
- (34) Chen, R.; Zhang, Y.; Xie, Q.; Chen, Z.; Ma, C.; Zhang, G. Transparent Polymer-Ceramic Hybrid Antifouling Coating with Superior Mechanical Properties. *Adv. Funct. Mater.* **2021**, 31, No. 2011145.
- (35) Golovin, K.; Boban, M.; Mabry, J. M.; Tuteja, A. Designing self-healing superhydrophobic surfaces with exceptional mechanical durability. *ACS Appl. Mater. Interfaces* **2017**, *9*, 11212–11223.
- (36) Hansen, C. M. Hansen solubility parameters: a user's handbook; CRC press: 2007; p. 151–174.
- (37) Lancaster, J. K. Abrasive wear of polymers. Wear 1969, 14, 223–239.
- (38) Shipway, P.; Ngao, N. Microscale abrasive wear of polymeric materials. *Wear* **2003**, 255, 742–750.
- (39) Bayart, E.; Svetlizky, I.; Fineberg, J. Slippery but tough: The rapid fracture of lubricated frictional interfaces. *Phys. Rev. Lett.* **2016**, *116*, No. 194301.

- (40) Hardy, W. B.; Doubleday, I. Boundary lubrication —The paraffin series. Proc. R. Soc. Lond. Ser. A 1922, 100, 550-574.
- (41) Bowden, F.; Gregory, J.; Tabor, D. Lubrication of metal surfaces by fatty acids. Nature 1945, 156, 97-101.
- (42) Bowden, F.; Tabor, D. The Friction and Imbrication Of Solids; Oxford, 2001; vol. 1, pp. 10 -32.
- (43) Kobayashi, M.; Terada, M.; Takahara, A. Reversible adhesivefree nanoscale adhesion utilizing oppositely charged polyelectrolyte brushes. Soft Matter 2011, 7, 5717-5722.
- (44) Millett, J. C. F.; Bourne, N. K.; Rosenberg, Z.; Field, J. E. Shear strength measurements in a tungsten alloy during shock loading. J. Appl. Phys. 1999, 86, 6707-6709.
- (45) Fischer, J.; Stawarzcyk, B.; Trottmann, A.; Hämmerle, C. H. F. Impact of thermal misfit on shear strength of veneering ceramic/ zirconia composites. Dent. Mater. 2009, 25, 419-423.
- (46) Ma, S.; Zhang, X.; Yu, B.; Zhou, F. Brushing up functional materials. NPG Asia Mater. 2019, 11, 24.
- (47) Peppou-Chapman, S.; Hong, J. K.; Waterhouse, A.; Neto, C. Life and death of liquid-infused surfaces: a review on the choice, analysis and fate of the infused liquid layer. Chem. Soc. Rev. 2020, 49, 3688-3715.
- (48) Chattopadhyay, D. K.; Raju, K. Structural engineering of polyurethane coatings for high performance applications. Prog. Polym. Sci. 2007, 32, 352-418.
- (49) Golovin, K.; Kobaku, S. P.; Lee, D. H.; DiLoreto, E. T.; Mabry, J. M.; Tuteja, A. Designing durable icephobic surfaces. Sci. Adv. 2016, 2, No. e1501496.
- (50) Benda, J.; Stafslien, S.; Vanderwal, L.; Finlay, J. A.; Clare, A. S.; Webster, D. C. Surface modifying amphiphilic additives and their effect on the fouling-release performance of siloxane-polyurethane coatings. Biofouling 2021, 37, 309-326.
- (51) Epstein, A. K.; Wong, T.-S.; Belisle, R. A.; Boggs, E. M.; Aizenberg, J. Liquid-infused structured surfaces with exceptional antibiofouling performance. Proc. Natl. Acad. Sci. U. S. A. 2012, 109, 13182-13187.
- (52) American Society for Testing and Materials (ASTM). Standard F3300-18, Standard Test Method for Abrasion Resistance of Flexible Packaging Films Using a Reciprocating Weighted Stylus; ASTM International: West Conshohocken, PA, 2018.
- (53) Liu, H.; Zhang, P.; Liu, M.; Wang, S.; Jiang, L. Organogel-based Thin Films for Self-Cleaning on Various Surfaces. Adv. Mater. 2013, 25, 4477-4481.
- (54) Yao, X.; Wu, S.; Chen, L.; Ju, J.; Gu, Z.; Liu, M.; Wang, J.; Jiang, L. Self-Replenishable Anti-Waxing Organogel Materials. Angew. Chem. Int. Ed. 2015, 54, 8975-8979.
- (55) Wang, J.; Lee, S.; Bielinski, A. R.; Meyer, K. A.; Dhyani, A.; Ortiz-Ortiz, A. M.; Tuteja, A.; Dasgupta, N. P. Rational Design of Transparent Nanowire Architectures with Tunable Geometries for Preventing Marine Fouling. Adv. Mater. Interfaces 2020, 7, No. 2000672.
- (56) Tesler, A. B.; Kim, P.; Kolle, S.; Howell, C.; Ahanotu, O.; Aizenberg, J. Extremely durable biofouling-resistant metallic surfaces based on electrodeposited nanoporous tungstite films on steel. Nat. Commun. 2015, 6, 8649.
- (57) Rosenhahn, A.; Sendra, G. H. Surface Sensing and Settlement Strategies of Marine Biofouling Organisms. Biointerphases 2012, 7, 63.
- (58) Golovin, K.; Dhyani, A.; Thouless, M.; Tuteja, A. Lowinterfacial toughness materials for effective large-scale deicing. Science **2019**, *364*, 371–375.
- (59) Golovin, K.; Tuteja, A. A predictive framework for the design and fabrication of icephobic polymers. Sci. Adv. 2017, 3, No. e1701617.
- (60) Painter, P. C.; Coleman, M. M. Fundamentals of polymer science: an introductory text; Technomic, 1997.

## **□** Recommended by ACS

## Insights into the Mechanical Properties of Ultrathin Perfluoropolyether-Silane Coatings

Oliver Zhao, Reinhold H. Dauskardt, et al.

MAY 11, 2022 LANGMUIR

READ 2

## A Lipid-Inspired Highly Adhesive Interface for Durable Superhydrophobicity in Wet Environments and Stable **Jumping Droplet Condensation**

Jingcheng Ma, Nenad Miljkovic, et al.

MARCH 11, 2022

ACS NANO

READ **C** 

## **Slippery Antifouling Polymer Coatings Fabricated Entirely from Biodegradable and Biocompatible Components**

Harshit Agarwal, David M. Lynn, et al.

APRIL 08, 2022

ACS APPLIED MATERIALS & INTERFACES

READ **C** 

## Non-wetting Liquid-Infused Slippery Paper

Saumyadwip Bandyopadhyay, Suman Chakraborty, et al.

NOVEMBER 09, 2021

LANGMUIR

READ **C** 

Get More Suggestions >